
Catch Your Breath: Adaptive Computation for Self-Paced Sequence Production

Alexandre Galashov*
Google DeepMind

Matt Jones
Google DeepMind

Rosemary Ke
Google DeepMind

Yuan Cao
Google DeepMind

Vaishnavh Nagarajan
Google DeepMind

Michael C. Mozer
Google DeepMind

Abstract

Within the landscape of inference-time scaling methods for foundation models, a *width-based* approach to scaling—which involves the insertion of `<PAUSE>` tokens in the input stream to delay model responses—offers a unique advantage by increasing model expressivity while remaining highly parallelizable at both training and inference. The existing literature on training models to utilize `<PAUSE>` tokens relies on the standard cross-entropy objective in which the model output is read out and evaluated only at the final step of a pause sequence. This approach provides no mechanism for the model to regulate its own processing or to signal readiness to respond, treating the additional compute steps as a static barrier rather than a resource to be used adaptively. We propose a supervised loss, *Catch Your Breath (CYB)*, framed as a sequential-decision problem, that trains a model to dynamically and autonomously scale the number of compute steps used for each input token. The model indicates the need for additional compute steps by emitting a special `<DON'T KNOW>` output, delaying its response via a pause. The model can abstain multiple times to obtain longer delays. Our experiments demonstrate that CYB significantly outperforms standard cross-entropy when introduced either in pretraining or fine-tuning, reducing perplexity and enhancing downstream accuracy with no additional computational or memory cost.

While remarkable advances in AI have been achieved by scaling model size and dataset size, a third scaling dimension has recently become a focus of intense interest: scaling the computational budget during inference. The most straightforward approach to inference-time scaling involves ‘thinking’ in some form, whether chain of thought [e.g., 43, 45, 47], repeated sampling, self critiques, or latent-thought methods [e.g., 15, 35, 38].

Inference-time scaling can also operate at a more granular level by boosting resources devoted to individual tokens, either by expanding model *depth* or model *width*. Depth-based approaches involve layer recurrence, i.e., repeating individual layers or a range of layers [e.g., 12]. Width-based approaches involve inserting special `<PAUSE>` tokens into the input stream [13]. Each `<PAUSE>` informs the model that it has an additional forward pass to perform further processing on the context and potentially improve the next token emitted.

Although depth-based approaches have gotten the bulk of notice in the literature (see Section 1), our work focuses on width-based approaches for they offer greater expressivity in a formal language sense [27, 30] and can be parallelized, unlike depth-based approaches that scale serially. However, in order to realize the potential of width-based approaches, our work aims to address a key limitation of the current literature, which we explain here. In width-based approaches, processing time is expanded for an input token by inserting one or more trailing `<PAUSE>` tokens, and when these tokens occur, the

*Address correspondence to {agalashov,mcmozer}@google.com

model output is ignored until the final pause step [13]. To appreciate the computational challenge this insertion poses for a transformer, consider an indexed token sequence such as

0:Donald, 1:lost, 2:his, 3:<pause>, 4:<pause>, 5:mind.

Without pauses, the model would be trained at step 2 to predict `mind`. With the pauses at steps 3 and 4, the model is trained to output `mind` at step 4 instead. However, because the model cannot anticipate that pauses will follow, it must act greedily and try to predict `mind` at step 2, which may deny it the opportunity to plan optimally with the additional computational steps. And even if it can predict well at step 2, the model must hold its response for two additional steps because producing `mind` at step 2 does not count as correct. These issues arise whether pauses are inserted randomly or systematically.

In this article, we propose to remedy the limitations of externally imposed delays in the input stream with a mechanism that allows the model itself to determine whether it wishes to pause. This method is inspired by studies of human reading, which find that readers fixate longer on words when processing demands rise (see Appendix [Appendix A](#)). For each input token, the model is given the option of emitting a special `<DON'T KNOW>` token to abstain from responding. With abstention, the arrival of further input is held off and the model is allowed an extra `<PAUSE>` step to continue processing (Figure 1a). The model can produce abstention responses multiple times in a row, yielding adaptive self-paced sequence production (Figure 1b).

To summarize our contributions: (1) We propose a principled loss, called *Catch Your Breath* or *CYB*, that trains a transformer to self-determine how many computation steps it requires for each input token. While most adaptive-computation techniques focus on inference acceleration, we show that training pause tokens with *CYB* yields uniformly superior performance compared to the existing (non-adaptive) method in the literature—applying the standard cross-entropy objective on the last pause step. (2) We propose a parallel training procedure for the *CYB* loss that is as compute and memory efficient as cross entropy. (3) We explore variants of the loss that include additional penalties for slow responses but find—consistent with our conjecture—that the *CYB* loss naturally drives the model to respond efficiently. (4) We show significant advantages of the *CYB* loss over cross entropy, both for models pretrained from scratch and models fine-tuned with `<PAUSE>` tokens, on both perplexity measures and downstream model performance. (5) We investigate where the model chooses to pause, and find systematic and intuitive insights into the model’s behavior.

1 Related research

Pause tokens. Prior work has proposed special content-free input tokens to improve model performance, variously referred to as ‘memory’ [5], ‘thinking’ [18], ‘dummy’ [24, Appendix A.3], ‘registers’ [9], and ‘filler’ [34] tokens. Goyal et al. [13] coined the term ‘pause’ tokens and focused on their role in granting models additional computation steps. Goyal et al. were the first to conduct extensive experiments with pretraining and fine-tuning, and subsequent work has utilized their paradigm. We will refer to their approach by the title of their paper, *Think Before You Speak* or *TBYS*. During pretraining, their data loader inserts W pauses into the text stream at uniformly random positions. When pauses are inserted, model outputs for the $W - 1$ steps leading up to the final pause token are ignored and excluded from the usual next-token-prediction cross-entropy loss. During fine-tuning, where a prefix sequence is given along with a target sequence, W' pauses are appended to the prefix, giving the model additional compute steps before its response. Goyal et al. found consistent benefits in downstream-task accuracy only when pauses were included in both pretraining and fine-tuning

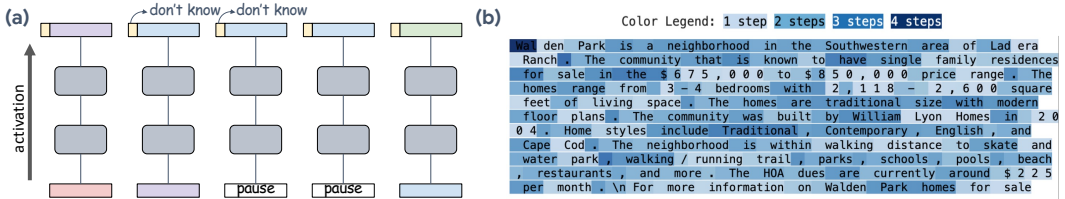


Figure 1: (a) Sequence processing in a transformer with `<DON'T KNOW>` outputs that trigger `<PAUSE>` inputs. (b) The *CYB* loss yields variable per-token computing steps. When the `<DON'T KNOW>` probability is high, additional computing steps are provided. Shading indicates the expected number of computing steps to predict the corresponding token.

stages. Although this approach appears to be an alternative to chain-of-thought methods, pauses may be related given that substituting meaningless filler tokens for the chain of thought still yields benefits [34]. In previous work, long delays are introduced between a prefix and a model’s response, intended to support explicit reasoning about and calculation of the response—an alternative to chain of thought. In contrast, our motivation is to allow short delays in processing any token, with the aim of facilitating integration of information in prefix tokens as well as in choosing any token in the response. Similar in spirit to our proposal, [10] propose an RL method that generates reasoning traces for individual tokens, also aimed at next-token prediction. The computational cost of our technique is significantly lower.

Anytime prediction and adaptive computation. In the anytime-prediction literature, models are tasked with making a series of responses that improve over time or with additional compute. Such models exhibit a *speed-accuracy* trade-off in which a coarse answer appears quickly but is refined with additional computation. In some schemes, the model is rewarded for getting the right response in as few steps as possible [e.g., 19]. Anytime prediction is related to adaptive computation-time for recurrent networks [14].

Adaptive depth models. Extending adaptive computation-time to transformers, *looped transformers* and variants have been proposed in which the functional depth of a model can be varied by repeating individual layers or ranges of layers [1, 3, 6, 11, 20, 23, 25, 29, 31, 32, 37, 44, 46, 50, 51]. Adaptation can be made on a per-token basis with a learned router.

<DON’T KNOW> outputs. The <DON’T KNOW> output is related to classification with abstention (or rejection) [4, 16, 26]. Two recent articles introduce heuristic notions of “I don’t know” to determine where pause tokens should be inserted. Cohen et al. [8] include a <DON’T KNOW> output and introduce a heuristic training objective that shifts probability to the <DON’T KNOW> output when the model predicts incorrectly. Their approach applies multiple heuristics to prevent the degenerate solution of always outputting <DON’T KNOW>. By integrating the <DON’T KNOW> option into our sequential-decision task, our approach does not suffer such degenerate solutions. Kim et al. [22] insert pause tokens when output entropy is high. This heuristic approach cannot distinguish aleatoric from epistemic uncertainty, which the CYB loss can in principle infer. Instead of assessing uncertainty at the token level, Manvi et al. [28] estimate a macro-level expected reward distribution via reserved outputs.

2 Optimizing compute steps with the Catch-Your-Breath (CYB) loss

In this section, we propose a loss that lets a transformer scale the number of compute steps used for individual tokens. (We refer the reader to the Table B.1 glossary if our notation becomes burdensome.)

In past research involving pause tokens, the *world* (i.e., data loader) determines how many transformer input steps are granted to each input token, denoted by random variable W , with $W \in \{1, 2, \dots, W^{max}\}$ and W^{max} is a fixed upper limit. This selection causes the insertion of $W - 1$ pauses in the input stream, and the model is tasked with producing an output token at the final step. With causal masking, the model gleans no information about the number of upcoming pauses. Consequently, it must be prepared to respond at each step where these additional pause tokens are inserted, leading to greedy optimization that may not best leverage the allocated compute time. Following [13], we refer to this state-of-the-art baseline approach as *Think Before You Speak (TBYS)*.

We hypothesize that pause steps might be better utilized if the model itself can control whether pauses are used. Our approach, CYB, assumes that each token is allowed the maximum number of steps, i.e., $W = W^{max}$. However, the model can choose to stop sooner: at each step $i < W$, the model can choose either to respond or to request an additional computation step via a <DON’T KNOW> response, chosen with probability $d_i \in [0, 1]$, which reflects the model’s desire to abstain. If the model chooses to respond or $i = W$ (the deadline is reached), a token is drawn from the usual next-token distribution, excluding <DON’T KNOW>.

We frame the selection of each individual output token as a sequential-decision problem, depicted in Figure 2. The subscripts in the Figure are a step index relative to the presentation of the real input token, $i \in \{1, 2, \dots, W^{max}\}$. The model has a sequence of decision points, indicated by the blue and purple boxes. At each step i , the model selects <DON’T KNOW> with probability d_i , a value that is dependent on model parameters and input. In accordance with the model’s confidence in its answer (probability $1 - d_i$), it selects an output token. The selected token will be either the target, with

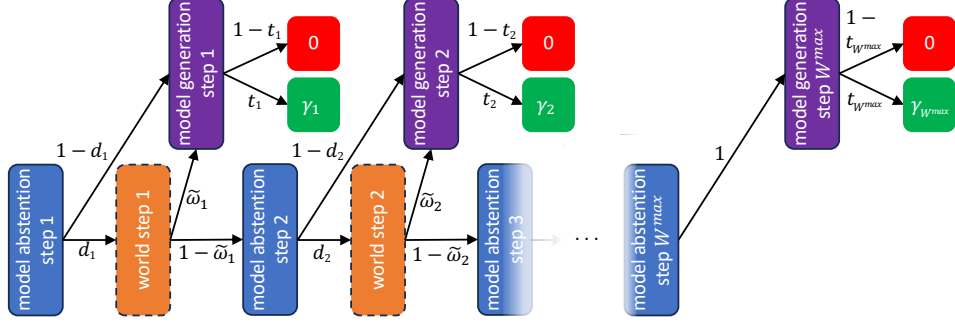


Figure 2: Catch Your Breath: A sequential-decision framework to obtain a single output token. The blue boxes represent model abstention decisions, the purple boxes model choices of output tokens. The orange boxes are choices made by the environment about whether the model is granted a delay in responding. The green and red boxes represent end-state rewards.

probability t_i , or an incorrect response, with probability $1 - t_i$. The green squares indicate the reward (accuracy) when correct, discounted by $\gamma_i \in [0, 1]$ at step i , and the red squares are the non-reward when incorrect.

In most experiments we conduct, models are allowed to use W^{max} steps per token. Our aim is to focus on the comparison of two alternative methods of training models to use the pauses, CYB and TBYS. However, to consider settings in which pauses are not distributed deterministically and uniformly (as the original TBYS formulated called for), we include a component, depicted by the orange boxes in Figure 2, which allows the world to force termination of processing and a read out. For such settings, we treat W as a random variable drawn from a categorical distribution parameterized by vector ω : $W \sim \text{Cat}(\omega)$. However, as stated above, we typically use $\omega = [0, 0, 0, \dots, 1]$ to allow the model to run for the maximum number of steps.

To incorporate the world termination actions into the sequential-decision framework of Figure 2, we rewrite the stop-probability priors, ω , as conditional probabilities, $\tilde{\omega}$, of terminating at step i given no previous termination, i.e.,

$$\tilde{\omega}_i \equiv \Pr(W = i \mid W \geq i) = \omega_i / \sum_{j=i}^{W^{max}} \omega_j \quad (1)$$

For a given token, the step at which the model must generate an output—self- or world-induced—is a random variable, S , with probability given by

$$\Pr(S = i \mid \mathbf{d}, \boldsymbol{\omega}) = \left(\omega_i + (1 - d_i) \sum_{j=i+1}^{W^{max}} \omega_j \right) \prod_{j=1}^{i-1} d_j \quad (2)$$

and $d_{W^{max}} \equiv 0$ for the final step. Equation (2) follows from Figure 2; Appendix Appendix G has a derivation.

The expected discounted accuracy obtained by the model in the CYB decision task is $\mathbb{E}_{i \sim \Pr(S \mid \mathbf{d}, \boldsymbol{\omega})} [\gamma_i t_i]$, which can be turned into a negative log likelihood loss:

$$\ell_{\text{CYB}}(\mathbf{t}, \mathbf{d}; \boldsymbol{\omega}, \boldsymbol{\gamma}) = -\log \mathbb{E}_{i \sim \Pr(S \mid \mathbf{d}, \boldsymbol{\omega})} [\gamma_i t_i]. \quad (3)$$

This loss is used to optimize model parameters via back propagation through the outputs \mathbf{t} and the <DON'T KNOW> probabilities, \mathbf{d} . It is conditioned on hyperparameters $\boldsymbol{\omega}$, the distribution over number of steps allotted for a token, and $\boldsymbol{\gamma}$, the vector of step-wise discount factors. The loss accommodates responses being read out at any step $i \in \{1, \dots, W^{max}\}$ with temporal discounting. The expectation in Equation 3 is computable by summing over the W^{max} steps to compute a mean of $\gamma_i t_i$ weighted by the probability in Equation 2.

The standard method of training <PAUSE> tokens, TBYS [13], is a special case of CYB with constant <DON'T KNOW> probabilities ($d_i = 1$ for $i < W$, $d_W = 0$), no discounting (i.e., $\gamma_i = 1$ for $i \in \{1, \dots, W^{max}\}$), and stop-probability priors, $\boldsymbol{\omega}$, corresponding to the manner in which tokens are inserted into the stream for training. For example, if two pauses are randomly inserted following 10% of real tokens, $W^{max} = 3$ and $\boldsymbol{\omega} = [.9, 0, .1]$.

CYB was motivated by a set of hypotheses, H1-H4, that we evaluate via simulation experiments.

- H1.** We conjecture that CYB will outperform TBYS when trained on identical data because CYB self-determines when to read out whereas TBYS lacks this control.
- H2.** CYB should yield a well calibrated model: to minimize the loss, the $\langle \text{DON'T KNOW} \rangle$ probability at step i , d_i , should be low when the target probability, t_i , is high and vice-versa. Further, the model should be time efficient: to minimize the CYB loss, the model should respond at step i unless the model’s response is likely to improve at step $i + 1$. Thus, it should not request all W^{\max} steps if not warranted by improved accuracy.
- H3.** Our hypothesis is that CYB’s benefit stems from its control over when to respond. Thus, if deadline uncertainty is added via the stop-time distribution, ω , CYB cedes some control (like TBYS), and we predict that accuracy will drop.
- H4.** The model’s speed-accuracy trade off can be shifted to allow the CYB-trained model to respond in fewer average steps at the expense of accuracy. We can impose a linear cost per step with, say, $\gamma_i = \gamma_0^{i-1}$ for hyperparameter γ_0 .

3 Methodology

Position encoding with pause sequences. To encode an input sequence, each token is assigned a position index which is used by positional embedding methods such as RoPE [40]. Treating $\langle \text{PAUSE} \rangle$ inputs like any other token will cause them to shift the position indices of following tokens. This approach was used by Goyal et al. [13], but may be problematic when introducing pauses during fine-tuning in a model that was trained without them. Consequently, we use RoPE but assign $\langle \text{PAUSE} \rangle$ tokens the same index as the immediately preceding non- $\langle \text{PAUSE} \rangle$ token. To ensure that the model can selectively index a specific pause token, we encode each pause in the sequence with a unique token code: $\langle \text{PAUSE1} \rangle$, $\langle \text{PAUSE2} \rangle$, etc.

Representing abstention. To obtain the $\langle \text{DON'T KNOW} \rangle$ output, d_i , we repurpose an unused token δ from the standard set of output alternatives and then renormalize the model’s output distribution, y , as $\hat{y}_{ij} = y_{ij}/(1 - y_{i,\delta})$ for token indices $j \neq \delta$, and $\hat{y}_{i,\delta} = 0$ otherwise. Whether fine-tuning or pretraining, we wanted to ensure a large enough $\langle \text{DON'T KNOW} \rangle$ prior probability that the model would learn to use it. We renormalized model posteriors to reflect a high prior for $\langle \text{DON'T KNOW} \rangle$, as detailed in Appendix [Appendix D](#).

Efficient training with CYB. Although the sequential-decision framework (Figure 2) might suggest training the model over sequential steps, we propose a procedure in which $W^{\max} - 1$ pauses are inserted into the input stream after each real input token during training. The transformer steps are run in parallel with causal masking. The pause steps may or may not be used by CYB, e.g., if at some step i the model is certain ($d_i \rightarrow 0$) or the world enforces a stop ($\tilde{\omega}_i \rightarrow 1$), the outputs at subsequent pauses will not contribute to the current token’s loss. During inference, when the transformer might be run autoregressively, we match the use of pauses at train time, i.e., always inserting $W^{\max} - 1$ pauses after each real input token. Because an input token and the pauses that follow can be processed in parallel, there is a trivial computational cost to inserting the maximum number of pauses in the stream for every token. Rather, the potential downside comes from the pauses cluttering the context window.

4 Results

We conducted experiments using Gemma1-2B [42] and Gemma3-4B [41], which we fine-tuned on a subset C4 [36]. We use sequences of 2048 real tokens which we expand to context windows of 4096, 6144, and 8192 tokens by inserting 1, 2, or 3 pauses following each real token, respectively. Unused token indices were repurposed to serve as pauses and $\langle \text{DON'T KNOW} \rangle$. Unless explicitly mentioned, all experiments conducted below use fine-tuned Gemma1-2B. Additionally, we conducted a pretraining experiment with Gemma1-2B using C4 [36]. Further details of the training procedure can be found in Appendix [Appendix D](#) and extended results in Appendix [Appendix F](#).

Our experiments focus on comparing two alternative losses for training a model with input $\langle \text{PAUSE} \rangle$ tokens: CYB, our method, and TBYS [13], which uses the standard cross-entropy loss and reads out the model’s response at the final $\langle \text{PAUSE} \rangle$. We match CYB and TBYS in the insertion of pauses, with $n \in \{1, 2, 3\}$ pauses after each real token. The methods differ only in the loss and the token-readout

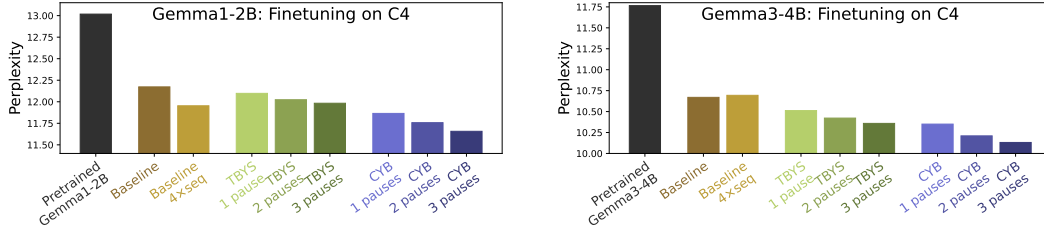


Figure 3: C4 evaluation set perplexity (lower is better) for pretrained Gemma1-2B (**left**) and Gemma3-4B (**right**) models (black bar) and various models fine-tuned on the C4 train set. Model variants include a baseline condition, where no modification is made to training objective or token sequence (brown bar), Think Before You Speak (TBYS) with 1, 2, and 3 pause tokens after each input token (green bars), and the CYB with 1, 2, and 3 pause tokens.

procedure. Compute and memory requirements are identical. Additionally, we train baseline methods on the same data *without the pauses* in order to show that pausing improves model quality. We can either match the baseline and pausing methods (CYB, TBYS) in terms of training data or compute. To match training data, we train a model referred to as *baseline* with a 2048 token context window. To match compute of the three-pause CYB and TBYS models, we train a model referred to as *baseline 4xseq* with an 8192 token context window which is filled with real data, providing it with fourfold advantage in data over the pausing methods.

Fine-tuning experiments. Figure 3 presents perplexity on a C4 evaluation set across different fine-tuned model variants. As one would expect, the pretrained model with no fine-tuning (black bar) has higher perplexity than the baseline model fine-tuned on C4 (brown bar). The light brown bar is a second baseline trained on sequences of length 8192 real tokens, which is compute matched to TBYS and CYB with three pauses. CYB consistently outperforms TBYS, to the point where 1-pause CYB beats 3-pause TBYS. The data-matched baseline (dark brown bar) has higher perplexity than any of the CYB and TBYS methods; the baseline that is compute matched to 3-pause TBYS/CYB (light brown bar) has higher perplexity than CYB with 1, 2, or 3 pauses.

Curiously, Goyal et al. [13] found that TBYS did not improve beyond baseline with fine-tuning. The difference might be explained by several adjustments to their methodology. We assign pause tokens distinct identities depending on their relative positions, and we use the same absolute sequence position for all pauses in a row. Further, we insert pause tokens systematically after every true input token, whereas Goyal et al. inserted them randomly and infrequently.

Pretraining experiment. We also conducted a pretraining experiment on C4, comparing TBYS and CYB with 3 pauses, with baselines included as a reference (Figure 4). As with fine-tuning experiments, we observe superior performance by both TBYS and CYB over the baselines, and CYB

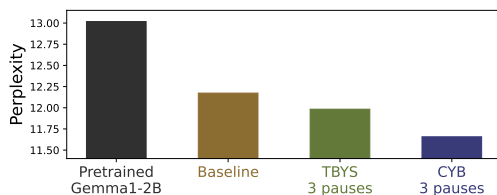


Figure 4: C4 evaluation set perplexity for Gemma1-2B architectures pretrained from scratch on C4 (except for the black bar, which uses open-source weights). Model variants include a baseline condition without pauses and models with three pauses per real token: TBYS [13] and CYB (ours).

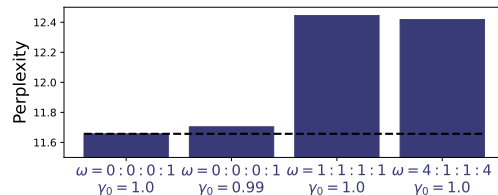


Figure 5: C4 evaluation set perplexity for various hyperparameters of CYB with Gemma1-2B fine-tuned on C4. Hyperparameter ω refers to the distribution of stopping times and is indicated by ratios for steps 0-3 (i.e., the initial input token and the following 3 pause tokens). Hyperparameter γ_0 refers to the discount factor. See Table B.1 for notation.

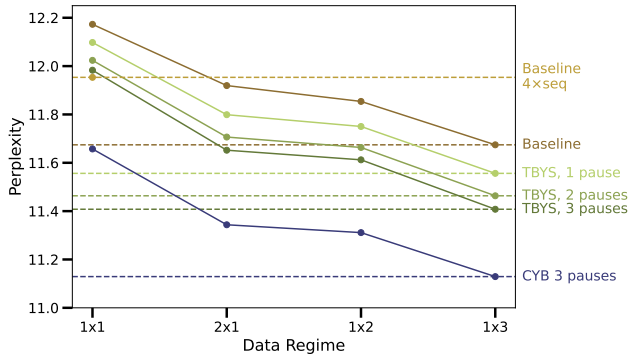


Figure 6: C4 evaluation set perplexity for various fine-tuned Gemma1-2B models based on a given data regime. 1×1 and 2×1 refer to 1 and 2 passes through the fine-tuning set, respectively. 1×2 and 1×3 refer to a single pass through 2 or 3 times the dataset size of 1×1 . The dashed lines indicate the perplexity of each model in the 1×3 training regime, except for *Baseline 4xseq* where we only report performance in the 1×1 regime.

delivers the strongest performance. CYB shows a larger benefit over TBYS in the pretraining setting relative to the fine-tuning setting: 3.6% lower perplexity for pretraining versus 2.7% for fine-tuning. (See Tables F.3 and F.4 in Appendix Appendix F.1.) Both the fine-tuning and pretraining experiments support our hypothesis **H1** that CYB outperforms TBYS. These methods are matched in memory, data, and computation and differ only in the loss function.

Data efficiency of CYB. While CYB reduces perplexity, developing intuitions about the significance of this reduction is challenging. We aim to offer such intuition by casting the improvement in terms of data efficiency. Figure 6 presents evaluation perplexity of various models fine-tuned in different data regimes. The regimes labeled 1×1 and 2×1 correspond to one and two passes through our 6.4M training sequences, respectively. The regimes labeled 1×2 and 1×3 correspond to data sets that are two and three times as large, respectively. CYB requires just 33% of the data to match baseline performance, and less than 66% of the data to beat performance of TBYS with three pauses. Interestingly, the performance gap between CYB and the alternative methods remains intact as data sets grow, indicating CYB’s gains are a genuine improvement in learning efficiency, not an artifact of data saturation. This experiment finds further support for hypothesis **H1**, the superiority of CYB over TBYS, here in data efficiency.

Hyperparameter exploration. We explored two hyperparameters of CYB introduced in Section 2: ω and γ_0 . Instead of allowing the three-pause CYB model to use as many steps as it wished, we imposed an external stop time distribution. We use the notation $\omega = \omega_1 : \omega_2 : \omega_3 : \omega_4$ to denote the ratio of probabilities of forcing the model to stop after processing steps 1-4. When CYB has full determination of when to stop within the pause sequence, $\omega = 0:0:0:1$. The other hyperparameter γ_0 , controls the exponential discounting of accuracy at each step (i.e., accuracy is discounted by γ_0^{i-1} at step i); $\gamma_0 = 1$ for no discounting.

Turning first to ω , Figure 5 shows perplexity for fine-tuned models with various hyperparameters and 3 pauses per token. The leftmost bar imposes no early stopping and no discounting—the result we previously presented. The rightmost two bars indicate performance when early stopping is imposed, either uniformly ($\omega = 1:1:1:1$) or with a bimodal distribution ($\omega = 4:1:1:4$). Consistent with **H3**, which posits that CYB’s advantage over TBYS stems from having control over when it responds, we see that losing this control via early stopping severely harms its performance.

In contrast, when discounting ($\gamma_0 = 0.99$) is applied, only a small cost in perplexity arises, as represented by the second bar from the left in Figure 5. Nonetheless, discounting is very effective in reducing the expected stopping step of the model, as indicated by the distribution shift between the first two columns of Figure 7. To explain these distributions, CYB’s `<DON’T KNOW>` output allows us to compute the *latency* distribution (Equation 2), i.e., the distribution over which step the model reads out its response. Figure 7 presents statistics of the latency distribution for four hyperparameter settings of CYB previously described in Figure 5. The blue curves are a probability density over the expected latency for individual tokens. The purple curves show the latency distribution averaged over tokens. The distributions in the first column ($\gamma_0 = 1$) shift leftward in the second column ($\gamma_0 = .99$), consistent with hypothesis **H4** that we can manipulate the model’s speed-accuracy trade off with discounting. With discounting, delaying a response is penalized unless the delay results in a corresponding boost in accuracy.

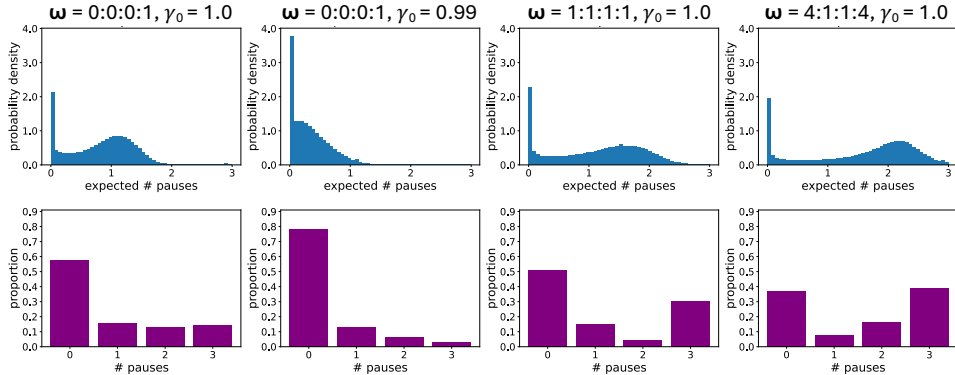


Figure 7: Latency distribution for four hyperparameter settings of CYB. Blue histograms show the distribution over evaluation tokens of the expected latency (the number of pause steps utilized). Purple bar graphs show the latency distribution averaged across tokens.

In the leftmost column of Figure 7, the model has no discounting penalty ($\gamma_0 = 1$) and need not accommodate forced stops ($\omega = 0:0:0:1$), yet CYB is nonetheless judicious in its use of pauses. This finding seems surprising given that additional pause steps should not *harm* performance. However, the finding is consistent with hypothesis **H3**, which asserts the advantage of CYB over TBYS is that CYB can stop when it is ready to respond instead of holding its response until the final step.

Paradoxically, forcing the model to stop early shifts its preferred latency distribution slower, as seen in last two columns of Figure 7. Perhaps the increased likelihood of `<DON'T KNOW>` is simply a reflection of its worse performance (Figure 5). We explored using soft constraints (secondary losses) to encourage the model to adhere to a target stop-time distribution, as an alternative to discounting. However, this approach yielded strictly worse performance from CYB. See Appendix [Appendix C](#) for details.

Calibration of model confidence and accuracy. If successful, CYB should train models to self-calibrate (Hypothesis **H2**): `<DON'T KNOW>` should have high probability when a delay in responding will improve model output. To be successful, the model must implicitly predict its own accuracy at subsequent steps and be sensitive to this prediction in using the `<DON'T KNOW>` output. Appendix [Appendix E](#) presents evidence showing a statistically reliable positive correlation between `<DON'T KNOW>` probability and an accuracy gain with additional processing for all steps of a three-pause model, supporting the calibration hypothesis **H2**.

Downstream task performance. We evaluate Gemma3-4B models fine-tuned on C4 with three pauses per token (zero for the baseline) on several downstream benchmarks: HellaSwag 10-shot [48], MMLU 5-shot [17], GSM8K 8-shot Chain of Thought (CoT) [7], reporting top-one accuracy in all cases. In these experiments, we insert three pauses after every real token for CYB and TBYS, including tokens in the prompt and in the response, both at fine-tuning and evaluation. For CYB, we generate responses by deterministic selection of the most probable response token, including `<DON'T KNOW>`. This procedure means that we run the sequential-decision framework selecting the most probable choice at every stage. For GSM8K, the C4 fine-tuned models achieved 0% accuracy in a zero-shot setting; we therefore additionally fine-tuned each model on the GSM8K training set for 2 epochs with a learning rate of $10^{-4}/\sqrt{d_{\text{model}}}$ and a warmup with 18 steps. Results are summarized in Table 1 and match results of perplexity analysis: CYB yields a consistent improvement in accuracy over TBYS, and both beat the baseline no-pause model.

Qualitative results. Table 2 shows pause-count statistics for selected tokens for the three-pause CYB model. The Table presents tokens which tend to be followed by few (*low median*) or many (*high median*) pauses, and those which tend to have the same number of pauses regardless of their context (*low variance*) or have context-sensitive pause durations (*high variance*). There are clear regularities in these tokens, such as the upper right cell being plural nouns, the upper left cell having highly predictable completions, and the lower left cell containing single letters.

Table 1: Downstream evaluation top-1 accuracy (%). HellaSwag and MMLU are evaluated on C4 fine-tuned checkpoints; GSM8K results are after additional fine-tuning on the GSM8K training set.

Method	HellaSwag (10-shot)	MMLU (5-shot)	GSM8K (8-shot)
Baseline	24.68	49.16	47.60
TBYS	24.74	52.70	53.37
CYB	27.94	54.00	53.67

Table 2: Statistics of pause counts for selected tokens following CYB training.

	Low Median	High Median
Low Variance	isn, wasn, didn, doesn, don, according, able, However, plenty, etc, Inc, &, non, addition	devices, players, students, projects, applications, challenges, environment, systems, stories, games, groups, events, patients, families, teams
High Variance	g, e, to, entry, S, won, co, New, Y, V, F, Z, World, of, Air	materials, images, @, site, pictures, photos, sites, code, College, wood, page, file, professionals, is, homes

Figure 1b presents a sample evaluation token sequence. Each token’s background is colored to indicate the expected number of pause steps requested by the model in order to predict that token. (That is, the coloring reflects the processing steps conditioned on the preceding token.) The coloring ranges from white to dark blue, corresponding to zero pause steps (1 total step) to 3 pause steps (4 total steps). The most obvious feature of the pause pattern is that it is not uniform but varies on a token-by-token basis. For example, the pause following the token ‘traditional’ in Figure 1b tends to be long; in contrast, the pause does not slow down when it is predicting a string of digits. More examples of shaded text can be found in Appendix Figures F.6 and F.7.

5 Discussion

We introduced Catch Your Breath (CYB), a sequential-decision framework and loss function that supports inference-time scaling of per-token computation. CYB requests additional compute steps when the output is uncertain, allowing it to delay its output and to pause the input sequence. In classical classification with abstention, epistemic uncertainty stems from data scarcity or gaps in training coverage. Under the CYB objective, however, uncertainty is fundamentally a reflection of computational constraints: the model is uncertain not because it lacks representation in its weights, but because it has not yet executed enough internal transformations to synthesize long-range context. As our calibration metrics show, subsequent pause steps allow the model to resolve this internal uncertainty, using test-time compute.

We described CYB as performing *width-based* scaling, which is an underexplored approach relative to *depth-based* scaling (e.g., looped transformers scaling by running layers multiple times). The existing paradigm used for width-based scaling, which we refer to as Think Before You Speak (TBYS), is a limiting case of CYB suffering from the fact that it lacks autonomy over the final readout point. We presented strong evidence that CYB outperforms TBYS (hypothesis **H1**), and that CYB’s benefit stems from its control over when to respond (hypothesis **H3**).

Although we demonstrated that CYB can be used to control the speed-accuracy trade off (hypothesis **H4**), it is important to emphasize that CYB is not motivated by raw inference-time compute savings; rather, it is about providing the architecture with flexible, context-dependent control over its computation. Just as human readers selectively modulate fixation durations to resolve lexical ambiguities or integrate complex discourse (see Appendix A), CYB-trained models naturally learn to pause only when the local transition dynamics demand it. This behavior is conceptually aligned with looped transformers that utilize internal routing components to decide whether or not to continue depth recurrence. However, width-based adaptation through CYB offers distinct structural and engineering advantages over these depth-recurrent models, including simplicity and elegance of the routing rule, parallelizability, and formal expressivity.

Limitations and future directions. The recipe we used for variable computation in CYB involves inserting the maximum number of pauses after each real token. While this recipe is highly parallelizable and introduces no computational or memory overhead *relative to TBYS*, it can limit the effective sequence length for long-form generation. This limit is the price of pause-based approaches like

CYB and TBYS relative to the baseline non-pause models. Future implementations could explore an alternative training recipe where variable numbers of pauses are inserted dynamically. This recipe is particularly well-suited for post-training alignment stages (such as RLHF or DPO) where autoregressive rollouts are standard, enabling insertion of a <PAUSE> only when an explicit <DON'T KNOW> is triggered. Other possible recipes exist, such as inserting pauses selectively at tokens most likely to benefit from them, as determined by analysis of trained models (e.g., Table 2).

Acknowledgments and Disclosure of Funding

We are grateful to the insights and assistance of Jasper Uijlings early in the course of this research.

References

- [1] Alabdulmohsin, I. and Zhai, X. (2025). Recursive inference scaling: A winning path to scalable inference in language and multimodal systems. In *The Thirty-ninth Annual Conference on Neural Information Processing Systems*.
- [2] Arnon, T. and Lavidor, M. (2023). Cognitive control in processing ambiguous idioms: evidence from a self-paced reading study. *Journal of Psycholinguistic Research*, 52(1):261–281.
- [3] Bae, S., Kim, Y., Bayat, R., Kim, S., Ha, J., Schuster, T., Fisch, A., Harutyunyan, H., Ji, Z., Courville, A., and Yun, S.-Y. (2025). Mixture-of-recursions: Learning dynamic recursive depths for adaptive token-level computation. In *The Thirty-ninth Annual Conference on Neural Information Processing Systems*.
- [4] Bartlett, P. L. and Wegkamp, M. H. (2008). Classification with a reject option using a hinge loss. *Journal of Machine Learning Research*, 9(59):1823–1840.
- [5] Burtsev, M. S., Kuratov, Y., Peganov, A., and Sapunov, G. V. (2021). Memory transformer.
- [6] Chen, Y., Shang, J., Zhang, Z., Xie, Y., Sheng, J., Liu, T., Wang, S., Sun, Y., Wu, H., and Wang, H. (2025). Inner thinking transformer: Leveraging dynamic depth scaling to foster adaptive internal thinking. arXiv:2502.13842 [cs.CL].
- [7] Cobbe, K., Kosaraju, V., Bavarian, M., Chen, M., Jun, H., Kaiser, L., Plappert, M., Tworek, J., Hilton, J., Nakano, R., Hesse, C., and Schulman, J. (2021). Training verifiers to solve math word problems.
- [8] Cohen, R., Dobler, K., Biran, E., and de Melo, G. (2024). I don't know: Explicit modeling of uncertainty with an [IDK] token. In *The Thirty-eighth Annual Conference on Neural Information Processing Systems*.
- [9] Darcet, T., Oquab, M., Mairal, J., and Bojanowski, P. (2024). Vision transformers need registers.
- [10] Dong, Q., Dong, L., Tang, Y., Ye, T., Sun, Y., Sui, Z., and Wei, F. (2025). Reinforcement pre-training. arXiv:2506.08007 [cs.CL].
- [11] Geiping, J., McLeish, S., Jain, N., Kirchenbauer, J., Singh, S., Bartoldson, B. R., Kailkhura, B., Bhatele, A., and Goldstein, T. (2025). Scaling up test-time compute with latent reasoning: A recurrent depth approach. arXiv:2502.05171 [cs.LG].
- [12] Giannou, A., Rajput, S., Sohn, J.-Y., Lee, K., Lee, J. D., and Papailiopoulos, D. (2023). Looped transformers as programmable computers. In Krause, A., Brunskill, E., Cho, K., Engelhardt, B., Sabato, S., and Scarlett, J., editors, *Proceedings of the 40th International Conference on Machine Learning*, volume 202 of *Proceedings of Machine Learning Research*, pages 11398–11442. PMLR.
- [13] Goyal, S., Ji, Z., Rawat, A. S., Menon, A. K., Kumar, S., and Nagarajan, V. (2024). Think before you speak: Training language models with pause tokens. In *ICLR*.
- [14] Graves, A. (2016). Adaptive computation time for recurrent neural networks. arXiv:1603.08983.

- [15] Hao, S., Sukhbaatar, S., Su, D., Li, X., Hu, Z., Weston, J., and Tian, Y. (2024). Training large language models to reason in a continuous latent space. arXiv:2412.06769 [cs.CL], also COLM 2025.
- [16] Hendrickx, K., Perini, L., Van der Plas, D., Meert, W., and Davis, J. (2024). Machine learning with a reject option: A survey. *Machine Learning*, 113(5):3073–3110.
- [17] Hendrycks, D., Burns, C., Basart, S., Zou, A., Mazeika, M., Song, D., and Steinhardt, J. (2020). Measuring massive multitask language understanding. *CoRR*, abs/2009.03300.
- [18] Herel, D. and Mikolov, T. (2023). Thinking tokens for language modeling (extended abstract). In *Eighth Conference on Artificial Intelligence and Theorem Proving (AITP 2023)*, Aussois, France.
- [19] Iuzzolino, M. L., Mozer, M. C., and Bengio, S. (2021). Improving anytime prediction with parallel cascaded networks and a temporal-difference loss. In Beygelzimer, A., Dauphin, Y., Liang, P., and Vaughan, J. W., editors, *Advances in Neural Information Processing Systems*.
- [20] Jeddi, A., Ciccone, M., and Taati, B. (2026). Loopformer: Elastic-depth looped transformers for latent reasoning via shortcut modulation. In *The Fourteenth International Conference on Learning Representations*.
- [21] Just, M. A. and Carpenter, P. A. (1980). A theory of reading: From eye fixations to comprehension. *Psychological Review*, 87(4):329–354.
- [22] Kim, E., Kim, S., and Thorne, J. (2025). Learning to insert [pause] tokens for better reasoning. arXiv:2506.03616 [cs.CL].
- [23] Koishikenov, Y., Lipani, A., and Cancedda, N. (2025). Encode, think, decode: Scaling test-time reasoning with recursive latent thoughts. arXiv:2510.07358 [cs.LG].
- [24] Lanchantin, J., Toshniwal, S., Weston, J., Szlam, A., and Sukhbaatar, S. (2023). Learning to reason and memorize with self-notes.
- [25] Li, Z., Li, Y., and Zhou, T. (2025). Skip a layer or loop it? test-time depth adaptation of pretrained llms. arXiv:2507.07996 [cs.LG].
- [26] Liu, Z., Wang, Z., Liang, P. P., Salakhutdinov, R. R., Morency, L.-P., and Ueda, M. (2019). Deep gamblers: Learning to abstain with portfolio theory. In Wallach, H., Larochelle, H., Beygelzimer, A., d’Alché Buc, F., Fox, E., and Garnett, R., editors, *Advances in Neural Information Processing Systems*, volume 32. Curran Associates, Inc.
- [27] London, C. and Kanade, V. (2025). Pause tokens strictly increase the expressivity of constant-depth transformers.
- [28] Manvi, R., Hong, J., Seyde, T., Labonne, M., Lechner, M., and Levine, S. (2025). Zero-overhead introspection for adaptive test-time compute.
- [29] McLeish, S., Li, A., Kirchenbauer, J., Kalra, D. S., Bartoldson, B. R., Kailkhura, B., Schwarzschild, A., Geiping, J., Goldstein, T., and Goldblum, M. (2025). Teaching pretrained language models to think deeper with retrofitted recurrence.
- [30] Merrill, W. and Sabharwal, A. (2025). A little depth goes a long way: The expressive power of log-depth transformers. arXiv:2503.03961 [cs.LG].
- [31] Ng, D. N. (2026). LLM neuroanatomy: How I topped the LLM leaderboard without changing a single weight. <https://dnhkng.github.io/posts/rys/>.
- [32] Nowak, A. I., Mercea, O.-B., Arnab, A., Pfeiffer, J., Dauphin, Y., and Evci, U. (2024). Towards optimal adapter placement for efficient transfer learning. arXiv:2410.15858 [cs.LG].
- [33] Oh, B.-D. and Schuler, W. (2022). Entropy- and distance-based predictors from GPT-2 attention patterns predict reading times over and above GPT-2 surprisal. In Goldberg, Y., Kozareva, Z., and Zhang, Y., editors, *Proceedings of the 2022 Conference on Empirical Methods in Natural Language Processing*, pages 9324–9334, Abu Dhabi, United Arab Emirates. Association for Computational Linguistics.

- [34] Pfau, J., Merrill, W., and Bowman, S. R. (2024). Let’s think dot by dot: Hidden computation in transformer language models. In *First Conference on Language Modeling*.
- [35] Phan, D., Hoffman, M. D., Dohan, D., Douglas, S., Le, T. A., Parisi, A., Sountsov, P., Sutton, C., Vikram, S., and Saurous, R. A. (2023). Training chain-of-thought via latent-variable inference. arXiv:2312.02179 [cs.LG].
- [36] Raffel, C., Shazeer, N., Roberts, A., Lee, K., Narang, S., Matena, M., Zhou, Y., Li, W., and Liu, P. J. (2020). Exploring the limits of transfer learning with a unified text-to-text transformer. *Journal of Machine Learning Research*, 21(140):1–67.
- [37] Rodkin, I., Orel, D., Smirnov, K., Bolatov, A., Elbouardi, B., Hassan, B., Kuratov, Y., Bulatov, A., Nakov, P., Baldwin, T., Shelmanov, A., and Burtsev, M. (2025). Beyond memorization: Extending reasoning depth with recurrence, memory and test-time compute scaling. arXiv:2508.16745 [cs.LG].
- [38] Ruan, Y., Band, N., Maddison, C. J., and Hashimoto, T. (2025). Reasoning to learn from latent thoughts. arXiv:2503.18866 [cs.LG].
- [39] Stewart, A. J., Kidd, E., and Haigh, M. (2009). Early sensitivity to discourse-level anomalies: Evidence from self-paced reading. *Discourse Processes*, 46:46–69.
- [40] Su, J., Lu, Y., Pan, S., Murtadha, A., Wen, B., and Liu, Y. (2023). Roformer: Enhanced transformer with rotary position embedding. arXiv:2104.09864 [cs.CL].
- [41] Team, G., Kamath, A., Ferret, J., Pathak, S., Vieillard, N., Merhej, R., Perrin, S., Matejovicova, T., Ramé, A., Rivière, M., Rouillard, L., Mesnard, T., Cideron, G., bastien Grill, J., Ramos, S., Yvinec, E., Casbon, M., Pot, E., Penchev, I., Liu, G., Visin, F., Kenealy, K., Beyer, L., Zhai, X., Tsitsulin, A., Busa-Fekete, R., Feng, A., Sachdeva, N., Coleman, B., Gao, Y., Mustafa, B., Barr, I., Parisotto, E., Tian, D., Eyal, M., Cherry, C., Peter, J.-T., Sinopalnikov, D., Bhupatiraju, S., Agarwal, R., Kazemi, M., Malkin, D., Kumar, R., Vilar, D., Brusilovsky, I., Luo, J., Steiner, A., Friesen, A., Sharma, A., Sharma, A., Gilady, A. M., Goedeckemeyer, A., Saade, A., Feng, A., Kolesnikov, A., Bendebury, A., Abdagic, A., Vadi, A., György, A., Pinto, A. S., Das, A., Bapna, A., Miech, A., Yang, A., Paterson, A., Shenoy, A., Chakrabarti, A., Piot, B., Wu, B., Shahriari, B., Petrini, B., Chen, C., Lan, C. L., Choquette-Choo, C. A., Carey, C., Brick, C., Deutsch, D., Eisenbud, D., Cattle, D., Cheng, D., Paparas, D., Sreepathihalli, D. S., Reid, D., Tran, D., Zelle, D., Noland, E., Huizenga, E., Kharitonov, E., Liu, F., Amirkhanyan, G., Cameron, G., Hashemi, H., Klimczak-Plucińska, H., Singh, H., Mehta, H., Lehri, H. T., Hazimeh, H., Ballantyne, I., Szpektor, I., Nardini, I., Pouget-Abadie, J., Chan, J., Stanton, J., Wieting, J., Lai, J., Orbay, J., Fernandez, J., Newlan, J., yeong Ji, J., Singh, J., Black, K., Yu, K., Hui, K., Vodrahalli, K., Greff, K., Qiu, L., Valentine, M., Coelho, M., Ritter, M., Hoffman, M., Watson, M., Chaturvedi, M., Moynihan, M., Ma, M., Babar, N., Noy, N., Byrd, N., Roy, N., Momchev, N., Chauhan, N., Sachdeva, N., Bunyan, O., Botarda, P., Caron, P., Rubenstein, P. K., Culliton, P., Schmid, P., Sessa, P. G., Xu, P., Stanczyk, P., Tafti, P., Shivanna, R., Wu, R., Pan, R., Rokni, R., Willoughby, R., Vallu, R., Mullins, R., Jerome, S., Smoot, S., Girgin, S., Iqbal, S., Reddy, S., Sheth, S., Pöder, S., Bhatnagar, S., Panyam, S. R., Eiger, S., Zhang, S., Liu, T., Yacovone, T., Liechty, T., Kalra, U., Evci, U., Misra, V., Roseberry, V., Feinberg, V., Kolesnikov, V., Han, W., Kwon, W., Chen, X., Chow, Y., Zhu, Y., Wei, Z., Egyed, Z., Cotruta, V., Giang, M., Kirk, P., Rao, A., Black, K., Babar, N., Lo, J., Moreira, E., Martins, L. G., Sansevierio, O., Gonzalez, L., Gleicher, Z., Warkentin, T., Mirrokni, V., Senter, E., Collins, E., Barral, J., Ghahramani, Z., Hadsell, R., Matias, Y., Sculley, D., Petrov, S., Fiedel, N., Shazeer, N., Vinyals, O., Dean, J., Hassabis, D., Kavukcuoglu, K., Farabet, C., Buchatskaya, E., Alayrac, J.-B., Anil, R., Dmitry, Lepikhin, Borgeaud, S., Bachem, O., Joulin, A., Andreev, A., Hardin, C., Dadashi, R., and Hussenot, L. (2025). Gemma 3 technical report.
- [42] Team, G., Mesnard, T., Hardin, C., Dadashi, R., Bhupatiraju, S., Pathak, S., Sifre, L., Rivière, M., Kale, M. S., Love, J., Tafti, P., Hussenot, L., Sessa, P. G., Chowdhery, A., Roberts, A., Barua, A., Botev, A., Castro-Ros, A., Slone, A., Héliou, A., Tacchetti, A., Bulanova, A., Paterson, A., Tsai, B., Shahriari, B., Lan, C. L., Choquette-Choo, C. A., Crepy, C., Cer, D., Ippolito, D., Reid, D., Buchatskaya, E., Ni, E., Noland, E., Yan, G., Tucker, G., Muraru, G.-C., Rozhdestvenskiy, G., Michalewski, H., Tenney, I., Grishchenko, I., Austin, J., Keeling, J., Labanowski, J., Lespiau, J.-B., Stanway, J., Brennan, J., Chen, J., Ferret, J., Chiu, J., Mao-Jones, J., Lee, K., Yu, K., Millican, K., Sjoesund, L. L., Lee, L., Dixon, L., Reid, M., Mikula, M., Wirth, M., Sharman, M., Chinaev, N.,

- Thain, N., Bachem, O., Chang, O., Wahltinez, O., Bailey, P., Michel, P., Yotov, P., Chaabouni, R., Comanescu, R., Jana, R., Anil, R., McIlroy, R., Liu, R., Mullins, R., Smith, S. L., Borgeaud, S., Girgin, S., Douglas, S., Pandya, S., Shakeri, S., De, S., Klimenko, T., Hennigan, T., Feinberg, V., Stokowiec, W., hui Chen, Y., Ahmed, Z., Gong, Z., Warkentin, T., Peran, L., Giang, M., Farabet, C., Vinyals, O., Dean, J., Kavukcuoglu, K., Hassabis, D., Ghahramani, Z., Eck, D., Barral, J., Pereira, F., Collins, E., Joulin, A., Fiedel, N., Senter, E., Andreev, A., and Kenealy, K. (2024). Gemma: Open models based on gemini research and technology.
- [43] Wei, J., Wang, X., Schuurmans, D., Bosma, M., Ichter, B., Xia, F., Chi, E., Le, Q., and Zhou, D. (2023). Chain-of-thought prompting elicits reasoning in large language models. arXiv:2201.11903 [cs.CL].
- [44] Yang, L., Lee, K., Nowak, R. D., and Papailiopoulos, D. (2024). Looped transformers are better at learning learning algorithms. In *The Twelfth International Conference on Learning Representations*.
- [45] Yao, S., Zhao, J., Yu, D., Du, N., Shafran, I., Narasimhan, K., and Cao, Y. (2023). React: Synergizing reasoning and acting in language models. arXiv:2210.03629 [cs.CL].
- [46] Yu, Z., Belinkov, Y., and Ananiadou, S. (2025). Back attention: Understanding and enhancing multi-hop reasoning in large language models. In Christodoulopoulos, C., Chakraborty, T., Rose, C., and Peng, V., editors, *Proceedings of the 2025 Conference on Empirical Methods in Natural Language Processing*, pages 11257–11272, Suzhou, China. Association for Computational Linguistics.
- [47] Zelikman, E., Wu, Y., Mu, J., and Goodman, N. D. (2022). Star: Bootstrapping reasoning with reasoning. arXiv:2203.14465 [cs.LG].
- [48] Zellers, R., Holtzman, A., Bisk, Y., Farhadi, A., and Choi, Y. (2019). HellaSwag: Can a machine really finish your sentence? *CoRR*, abs/1905.07830.
- [49] Zellner, A. (1988). Optimal information processing and Bayes’s theorem. *The American Statistician*, 42(4):278–280.
- [50] Zeng, B., Song, S., Huang, S., Wang, Y., Li, H., He, Z., Wang, X., li, Z., and Lin, Z. (2026). PonderLM: Pretraining language models to ponder in continuous space. In *The Fourteenth International Conference on Learning Representations*.
- [51] Zhu, R.-J., Wang, Z., Hua, K., Zhang, T., Li, Z., Que, H., Wei, B., Wen, Z., Yin, F., Xing, H., Li, L., Shi, J., Ma, K., Li, S., Kergan, T., Smith, A., Qu, X., Hui, M., Wu, B., Min, Q., Huang, H., Zhou, X., Ye, W., Liu, J., Yang, J., Shi, Y., Lin, C., Zhao, E., Cai, T., Zhang, G., Huang, W., Bengio, Y., and Eshraghian, J. (2025). Scaling latent reasoning via looped language models. arXiv:2510.25741 [cs.LG].

Appendix A How people read

The inspiration for this research comes from studies of human reading. When gaze is tracked as an individual reads, inter-saccade durations are highly nonuniform. Readers fixate longer when processing demands rise, e.g., at points where information can be integrated across phrases, where inferences can be made at the end of sentences, and where low-frequency terms occur [21]. Figure A.1 shows fixation order within a sentence for a human reader as well as the fixation duration. Note that short function words are skipped or quickly glanced over. When an uncommon interpretation of a word or sentence is required, readers pause. For instance, when idioms that typically have a figurative meaning (e.g., ‘break the ice’) are used in a literal way, processing time slows at the point where the disambiguating information is provided [2]. Similarly, readers pause when anomalous or unexpected information is provided, including attributes and spatial position of a character or object [39]. These various results suggest that people integrate information in an ongoing manner, where each incoming word and clause is processed with respect to prior context, and reading time is governed by the computational demands of online evaluative processes.

In humans, the ongoing, word-by-word integration processes might be described as *microinference*, in contrast to *macroinference*, which involves solving complex reasoning and planning problems. In AI, past research on pause tokens has focused on their utility for macroinference [13, 18, 22, 34]. Our present work is aimed at emphasizing the role of delays for microinference, motivated by the need to integrate and interpret information in an ongoing fashion. One important clue that this focus will be productive comes from a study which found that GPT-2 attention patterns could predict human reading times, in particular measures of the dispersion of attention and the change in attention patterns across time steps [33].

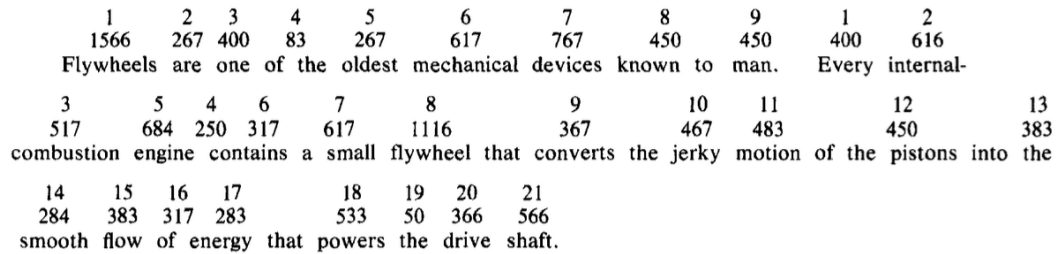


Figure A.1: Gaze fixations of a human reader. Indices indicate order of gaze within a sentence along with fixation duration (in msec). Reprinted from [Just and Carpenter \(1980, Figure 1\)](#).

Appendix B Notation used in the main article

Table B.1: Notation Used in the Main Article

Term	Meaning
W^{max}	maximum number of steps granted by world for any token
W	r.v. denoting # steps granted by world for a specific token, $1 \leq W \leq W^{max}$
S	r.v. denoting # steps at which model generates result (either by world or model $\langle \text{DON'T KNOW} \rangle$), $1 \leq S \leq W^{max}$
ω_i	prob. that world terminates processing at step i , $\Pr(W = i)$
$\tilde{\omega}_i$	prob. that world terminates processing at i given no prior termination, $\Pr(W = i W \geq i)$
d_i	prob. of model abstention ($\langle \text{DON'T KNOW} \rangle$) at step i
s_i	prob. of outputting result (self- or world-induced) at step i ; shorthand for $\Pr(S = i)$
t_i	prob. that the model selects ground-truth token at step i
γ_i	discount factor on accuracy at step i , $0 \leq \gamma_i \leq 1$
γ_0	hyperparameter for exponential discounting, with $\gamma_i = \gamma_0^{i-1}$
ρ_i	[CYB-VA, CYB-DP] prior prob. of self-induced termination at step i
α	[CYB-DP] penalty coefficient on prior-distribution mismatch

Appendix C Guiding CYB to obtain a desired stop-time distribution

We describe two variants of CYB that impose an additional constraint on model outputs with the goal of obtaining a desired stop-time distribution. We refer to this target distribution as ρ .

Appendix C.1 Variational approach (CYB-VA)

This approach aims to obtain a desired distribution ρ and to minimize the loss with respect to this distribution, i.e.,

$$\ell_{\text{CYB}\rho} = -\log \mathbb{E}_{i \sim \text{Cat}(\rho)} [\gamma_i t_i].$$

However, this loss does not depend on \mathbf{d} and will thus fail to train the $\langle \text{DON'T KNOW} \rangle$ output, let alone train it to be consistent with ρ . To achieve this goal, we take a variational approach and train the model using the ELBO. Treating the model’s likelihood at step i as the penalized value $\Pr[\text{target} | S = i] = \gamma_i t_i$, the ELBO is the right hand side of the inequality:

$$\log \mathbb{E}_{i \sim \text{Cat}(\rho)} [\gamma_i t_i] \geq \mathbb{E}_{i \sim \text{Cat}(\mathbf{s})} \log [\gamma_i t_i] - D_{\text{KL}}(\mathbf{s} || \rho)$$

where we assume as before that externally induced stops are eliminated. The $\langle \text{DON'T KNOW} \rangle$ distribution, \mathbf{d} , is incorporated via the stopping time distribution $\mathbf{s} \equiv \Pr(S | \mathbf{d})$ (Equation 2). We then define a negative ELBO loss,

$$\ell_{\text{CYB-VA}} = -\mathbb{E}_{i \sim \text{Cat}(\mathbf{s})} \log [\gamma_i t_i] + D_{\text{KL}}(\mathbf{s} || \rho).$$

Minimizing $\ell_{\text{CYB}\rho}$, as an upper bound on our desired loss, trains the model’s predictions (\mathbf{t}) by optimizing the expected discounted likelihood under \mathbf{s} . It also trains the model’s stopping time distribution (\mathbf{s}) toward the posterior, following the optimization view of Bayesian inference [e.g., 49]. We can determine the equilibrium self-stop distribution by taking the gradient of the variational loss,

$$\nabla_{\mathbf{s}} \ell_{\text{CYB-VA}} = -\log \gamma - \log \mathbf{t} - \log \rho + \log \mathbf{s} + \mathbf{1}.$$

Introducing a Lagrange multiplier for the constraint $\sum_i s_i = 1$ yields the optimality condition $\log \mathbf{s} = \log \gamma + \log \mathbf{t} + \log \rho - (\lambda + 1)\mathbf{1}$, resulting in $s_i \propto \rho_i \gamma_i t_i$. The model will thus learn to stop at times when both the stopping prior and its discounted accuracy are high. This analysis also indicates that the prior, ρ , and the discount factors, γ , are redundant in CYB-VA. We thus assume $\gamma_i = 1$ in all experiments with CYB-VA. CYB-VA thus has hyperparameters ρ , in addition to specifying W^{max} , the upper limit on the number of steps.

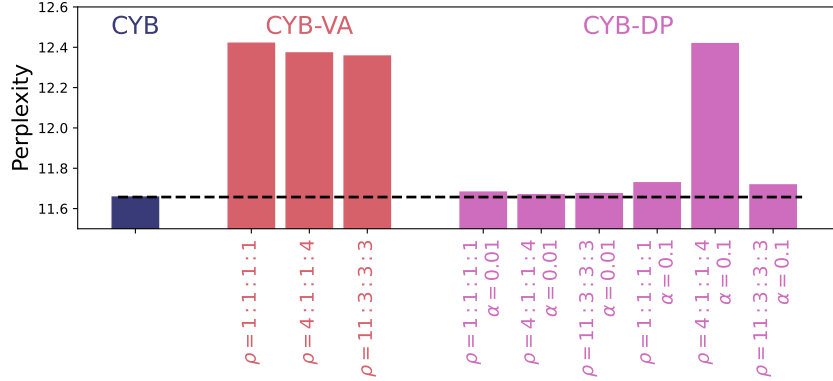


Figure C.2: C4 evaluation set perplexity for various hyperparameter settings of CYB and two variants, CYB-VA and CYB-DP, on Gemma1-2B fine-tuning experiment. The black dashed line indicates the perplexity of CYB. Hyperparameters ρ refer to the distribution of stopping times and are indicated by ratios for steps 0-3 (i.e., the initial input token and the following 3 pause tokens). Hyperparameter α is a penalty term associated with CYB-DP. See Table B.1 for notation.

Appendix C.2 Distributional penalty (CYB-DP)

A final approach is to optimize for our original loss, ℓ_{CYB} (Equation 3), and impose a penalty based on the deviation of the model’s desired and observed stop-time distributions:

$$\ell_{\text{CYB-DP}} = \ell_{\text{CYB}} + \alpha D_{\text{KL}}(\rho \parallel s),$$

where α specifies a penalty on the distribution mismatch. Note that the direction of the KL terms is reversed for $\ell_{\text{CYB-DP}}$ versus $\ell_{\text{CYB-VA}}$, in order to strongly penalize stopping times that are outside the support of the prior. (And we wish to allow the prior to have zero values.) CYB-DP has hyperparameters ρ and α , in addition to specifying W^{max} , the upper limit on the number of steps.

Appendix C.3 Results from CYB-VA and CYB-DP simulations

Perplexity. Figure C.2 shows perplexity for CYB, three hyperparameter settings for CYB-VA and six for CYB-DP on Gemma1-2B fine-tuning experiment. CYB-VA performs poorly for three different target stop-time distributions, ρ . We considered incorporating a scaling coefficient on the KL term, but CYB-VA’s elegance stems from the fact that such a coefficient should not be required. For CYB-DP, which penalizes deviation from a target stop-time distribution, we tested two penalty coefficients, α , and three target distributions, ρ . The smaller penalty yielded better performance, and the similar performance over ρ suggests that the penalty had little impact. If the penalty is not shaping learning, CYB-DP becomes equivalent to CYB with no world-induced early stopping.

Distributions of stopping times. Stopping-time distributions for CYB-DP and CYB-VA are presented in Figures C.3 and C.4. These Figures are analogous to Figure 7 from the main paper. CYB-VA adheres to the prior distribution and in general shows little variance indicating that it is insensitive to the specific token and context, which is a bad sign for an adaptive-pause method. CYB-DP for large $\alpha = 0.1$ behaves closer to CYB-VA and for smaller $\alpha = 0.01$ prefers longer latencies than CYB. However, longer latencies do not result in a lower perplexity compared to CYB.

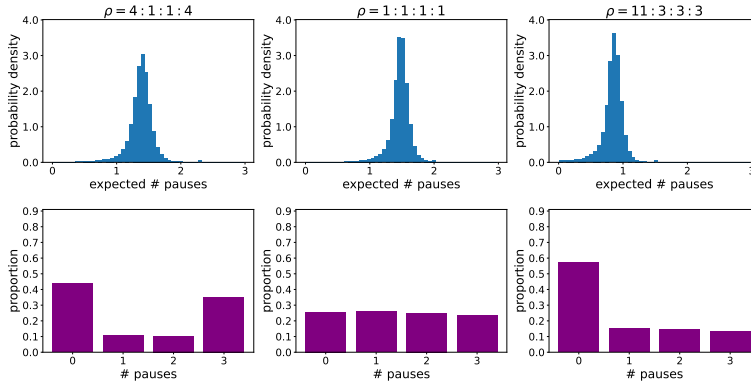


Figure C.3: Distribution of stopping times for CYB-VA. Blue histograms show the distribution over evaluation tokens of the expected number of pause steps. Purple bar graphs show the distribution over the number of pause steps across tokens.

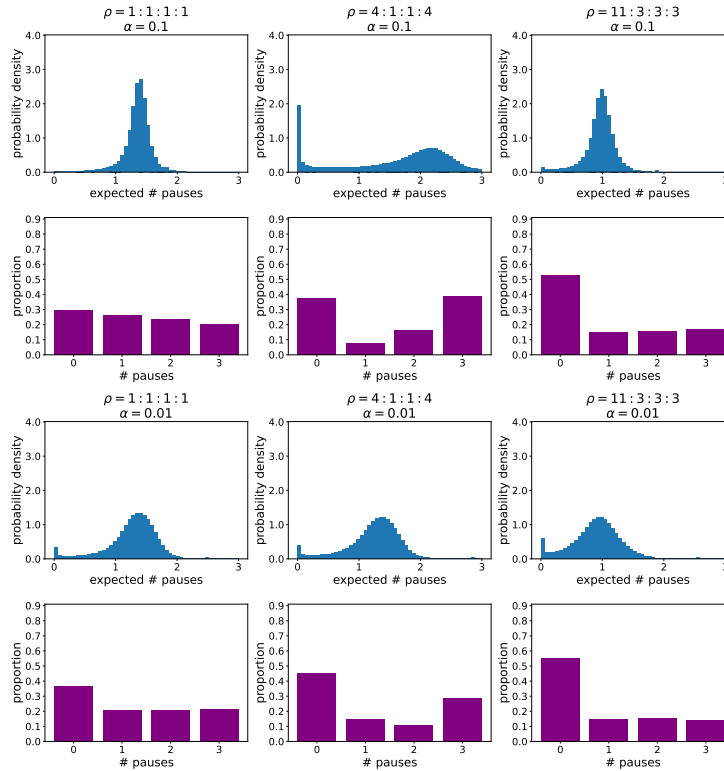


Figure C.4: Distribution of stopping times for CYB-DP with $\alpha = 0.1$ and $\alpha = 0.01$. Blue histograms show the distribution over evaluation tokens of the expected number of pause steps. Purple bar graphs show the distribution over the number of pause steps across tokens.

Appendix D Additional methodology

Appendix D.1 Training hyperparameters and data

For all the fine-tuning experiments, we fine-tuned either Gemma1-2B or Gemma3-4B models on a subset of 6.4 millions of sequences of the C4 dataset. For Gemma1-2B model we used batch size of 256, leading to a total of $25k$ iterations, while for Gemma3-4B model we used batch size of 64 leading to a total of 100k iterations. For pretraining experiments, we trained from scratch Gemma1-2B with batch size of 256 on 56×6.4 millions of sequences of the C4 dataset. For the evaluation, we use 160K sequences (59.8M tokens) from the C4 validation set.

We use a “concatenate then split” packing algorithm and a cosine learning rate decay with a linear warmup. We select a constant α and produce maximum value of learning rate by dividing it by the square root of model embedding dimension. The minimum value of learning rate is given by a maximum value multiplied by 10^{-2} . Before running all the experiments, we ran a sweep over $\alpha \in [10^{-2}, 5 \times 10^{-3}, 10^{-3}, 5 \times 10^{-4}, 5 \times 10^{-5}, 10^{-5}, 10^{-6}]$ where we ran the fine-tuning experiment on Gemma1-2B with baseline, TBYS with 3 pauses and CYB with 3 pauses. We found that $\alpha = 10^{-4}$ gave overall the best results for all the methods and this is what we used.

All the experiments are conducted on TPUv5 hardware.

Appendix D.2 Initializing <DON'T KNOW>

Because the pretrained model was never rewarded for assigning probability mass to the <DON'T KNOW> token, we wanted to ensure that the model actually had the potential to output <DON'T KNOW> when being fine-tuned with the CYB loss. To achieve this objective, model posteriors were renormalized to reflect a high prior for <DON'T KNOW>. If ψ is the prior distribution over tokens during pretraining and ψ' is the prior we wish to be reflected in the model posteriors, we add $\log(\psi'/\psi)$ to the model logit vector. With uniform pretraining priors, i.e., $\psi_i = 1/|V|$ with V being the vocabulary, we set ψ'_{DK} for the <DON'T KNOW> and $\psi'_i = (1 - \psi'_{DK})/(|V| - 1)$ for all other indices i . In the reported experiments, we use $\psi'_{DK} = 0.9$. We found the models trained better with $\psi'_{DK} \geq 0.9$.

Comparison models. Our primary aim is to argue that CYB outperforms the memory- and compute-matched TBYS in its ability to utilize <PAUSE> tokens. TBYS is identical but is trained by the ordinary cross-entropy loss. For TBYS, we used the same position coding scheme as in the CYB models, even though the original TBYS model treated pauses like any other token for the purpose of position coding. (The original TBYS model also does not encode the first, second, etc. pause in sequence distinctly from the others.) We varied the number of pauses after each real token from one to three for both CYB and TBYS. Evaluation of all comparison models and CYB used the same subset of 160k sequences from a validation set of C4.

Baselines. We tested a *baseline* model with no pause tokens inserted in the sequences. The baseline model thus had the same number of real tokens per input sequence but $1/W^{max}$ the overall length of the CYB and TBYS models with $W^{max} - 1$ pauses. Thus, the baseline is data matched but lower in memory and compute demands. We included a second baseline, which we refer to as *baseline 4xseq*, which is memory and compute matched but its context window is filled with $W^{max} = 4$ times as many training tokens as CYB and TBYS.

Additional fine-tuning data regimes. Besides the original fine-tuning regime, we ran a subset of methods (baselines and CYB) using $2\times$ and $3\times$ training data as well as using 2 epochs on the original dataset.

Appendix D.3 Where and how many pauses are permitted?

Two distinct recipes can be used for training with the CYB losses. We use the first of these, but future research could explore the second. Both require that we specify the maximum number of pause steps allowed, W^{max} .

Appendix D.3.1 Recipe 1: Constant number of pauses

The first recipe, which we use in the experiments we report in the main paper, inserts W^{max} pauses in the input stream after each real input token during training. The transformer steps are run in parallel with causal masking. The pause steps may or may not be used by the model, e.g., if at some step i the model is certain ($d_i \rightarrow 0$) or the world enforces a stop ($\omega_i \rightarrow 1$), the outputs at subsequent pauses will not contribute to the loss.

During inference, when the transformer might be run autoregressively, we match the use of pauses at train time, i.e., always inserting W^{max} pauses after each real input token. Because an input token and the pauses that follow can be processed in parallel, there is no computational cost to inserting the maximum number of pauses in the stream for every token. Rather, the potential cost comes from the pauses cluttering the context window. Even when W^{max} pauses are inserted at both training and inference, and even when the model is not pressured to reply quickly (e.g., $\gamma_i = 1$ for all i), the model must still learn to use the `<DON'T KNOW>` output to calibrate itself and determine when to read out.

Appendix D.3.2 Recipe 2: Variable number of pauses

The second recipe involves a variable number of pause steps at both training and inference. The CYB losses can accommodate variability in the number of pauses following a token at training. No modification to the loss needs be made, but the `<DON'T KNOW>` probability must be forced to zero on the last pause, or in response to an input token itself when there are no pauses. Rather than computing the expectation over world stopping times, we can sample a stopping time for each token and insert that number of pause steps in the input stream. One might also envision training methods that insert more pauses where they are likely to be most useful, e.g., where thinking might be required. (In the results section, we present evidence that pause requests by the model are token- and context-specific.)

During inference, the transformer might be run autoregressively, and we can again sample from the world stop-time distribution to determine the number of pause steps, and sample from the model’s `<DON'T KNOW>` confidence to determine which of the allowed steps to read out from.

Appendix E Calibration of model confidence and accuracy

If successful, CYB should train models to self-calibrate: `<DON'T KNOW>` should have high probability when a delay in responding will improve model output. To be successful, the model must implicitly predict its own accuracy at subsequent steps. That is, the probability of responding `<DON'T KNOW>` at step i , d_i , should be large when the target probability is higher at the next step, i.e., $t_{i+1} > t_i$. Figure E.5 shows joint density maps of `<DON'T KNOW>` probability (along ordinate) and the improvement in accuracy obtained by a one-step delay in responding (along abscissa). The three density maps correspond to steps $i \in \{0, 1, 2\}$. A positive correlation indicates that the model can predict when it will benefit by the delay. Over the evaluation set, the Spearman correlation coefficient between d_i and $t_{i+1} - t_i$ is 0.383, 0.157, and 0.271 for steps 0-2, respectively, all reliably nonzero ($p < 0.001$). The correlations are only slightly stronger with the discounting variant of CYB ($\gamma = 0.99^{\{0,1,2,3\}}$)—0.381, 0.208, and 0.309—indicating that penalizing delayed responses does not appear to make the model much better at determining when to pause.

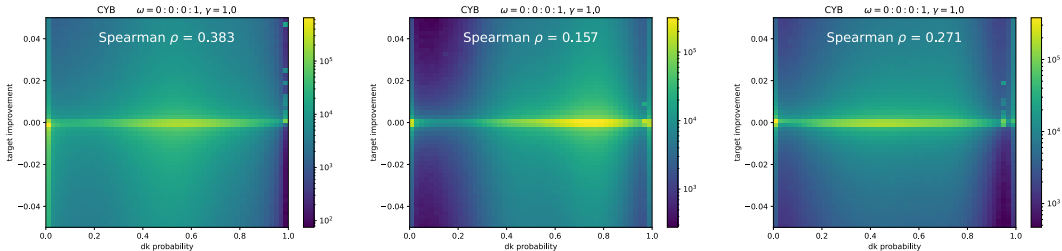


Figure E.5: Density plots indicating that `<DON'T KNOW>` probability is positively correlated with improvement in accuracy, for steps 0, 1, and 2.

Appendix F Additional results

In this section, we present additional results.

Appendix F.1 Tabular representations of the results from the main paper

In this section, we present the results from Figure 3 and Figure 4 in a tabular format for the easy introspection. We report C4 eval set perplexity as well as the relative perplexity improvement (in %) compared to the baseline perplexity. Relative improvement is computed as the percentage decrease in perplexity relative to the TBYS with 3 pause tokens, i.e.

$$\text{Relative Improvement} = (\text{PPL}_{\text{TBYS},p=3} - \text{PPL}_{\text{method}}) / \text{PPL}_{\text{TBYS},p=3} \times 100\% \quad (4)$$

The results for fine-tuning of Gemma3-4B model are given in Table F.2. We see that even CYB with 1 pause outperforms TBYS with 3 pauses. Using 3 pauses with CYB improves performance even further leading to **+2.2%** relative improvement in perplexity. The results for fine-tuning of Gemma1-2B model are given in Table F.3. Overall, the behavior is very similar to Gemma3-4B experiment. Finally, the results of pretraining of Gemma1-2B model are given in Table F.4. What is remarkable is that using CYB with pretrained model leads to even higher relative improvement in perplexity, notably **+3.57%** compared to the fine-tuned model which enjoys **+2.72%** relative improvement.

Method	Perplexity	Rel. Improvement (%)
Pretrained Gemma3-4B	11.765	-13.57%
Baseline	10.670	-3.00%
Baseline 4×seq	10.694	-3.24%
TBYS 1 pause	10.512	-1.48%
TBYS 2 pauses	10.422	-0.61%
TBYS 3 pauses	10.359	—
CYB 1 pauses	10.351	+0.08%
CYB 2 pauses	10.210	+1.44%
CYB 3 pauses	10.131	+2.20%

Table F.2: **Results for fine-tuned (on C4) Gemma3-4B.** Perplexity on eval set of C4. For relative improvement, we use the formula (4). In **bold** we highlight the best result – the lowest perplexity and the highest relative improvement.

Method	Perplexity	Rel. Improvement (%)
Pretrained Gemma1-2B	13.018	-8.64%
Baseline	12.173	-1.58%
Baseline 4×seq	11.953	+0.25%
TBYS 1 pause	12.098	-0.96%
TBYS 2 pauses	12.024	-0.34%
TBYS 3 pauses	11.983	—
CYB 1 pauses	11.865	+0.99%
CYB 2 pauses	11.758	+1.88%
CYB 3 pauses	11.657	+2.72%

Table F.3: **Results for fine-tuned (on C4) Gemma1-2B.** Perplexity on eval set of C4. For relative improvement, we use the formula (4). In **bold** we highlight the best result – the lowest perplexity and the highest relative improvement.

Method	Perplexity	Rel. Improvement (%)
Pretrained Gemma1-2B	13.018	-4.14%
Baseline	12.893	-3.14%
TBYS 3 pauses	12.500	—
CYB 3 pauses	12.054	+3.57%

Table F.4: **Results for trained from scratch (on C4) Gemma1-2B**. Perplexity on eval set of C4. For relative improvement, we use the formula (4). In **bold** we highlight the best result – the lowest perplexity and the highest relative improvement.

When you mute iOS, incoming phone calls and texts vibrate instead of playing whatever ringtone you set up. Alarms, on the other hand, will always play the ringtone whether your phone is muted or not. If you'd like to be able have an alarm vibrate your device instead of making a sound, you can do that by creating a silent ringtone. \n Adding custom ringtones to your iOS device is not difficult. Unfortunately, there are no silent ringtones built in. There are a few available in the Apple Store for purchase, and if you want to add a new ringtone without hooking your phone up to a computer and using iTunes, purchasing one from the store is the only easy way to do it. \n If you are willing to use iTunes, you have other options. You can make your own silent ringtone using a program like Audacity or a ringtone creator app on your phone – just record a few seconds of silence. But that's still a bit of a hassle, so we created this silent ringtone to save you the trouble. \n Just download the file, unzip it, then drag the file to iTunes (or open the file from within iTunes). iTunes will know that it's a ringtone because it uses the M4R file extension and will set it up where it needs to go. Connect your device to your computer and open the device settings in iTunes. \n On the Tones page, make sure "Sync Tones" is enabled, then choose whether you want to sync all tones or just selected tones. \n Sync your device with iTunes and the ringtone will now be available on your device. \n Now that you have the silent ringtone on your device, you can set it up with an alarm. Open your clock App and switch to the Alarm tab. \n Tap the New button to create a new alarm. \n Set the time and other options for your new alarm and then tap Sound. \n On the Sound page, your custom ringtones are listed at the top of the available ringtones. Select your new silent ringtone (your phone will vibrate when you do) and then tap Back. \n Tap Save to save your new silent alarm. \n Now, whether your device is muted or not, that alarm will only vibrate and will not make any sound. \n That's all there is to it. Yes, you have to deal with iTunes, but only briefly. And once you've got the silent ringtone installed, you'll probably find other uses for it as well. For example, you could assign it to specific contacts if

Color Legend: 1 step 2 steps 3 steps 4 steps

Figure F.6: Model trained with CYB loss produces variable pause durations on tokens.

Appendix G Derivation of output probability

Based on Figure 2, the probability of outputting a result at step i is given by

$$\Pr(S = i | \mathbf{d}, \boldsymbol{\omega}) = \left(\prod_{j=1}^{i-1} d_j \right) \left(\prod_{j=1}^{i-1} (1 - \tilde{\omega}_j) \right) (d_i \tilde{\omega}_i + (1 - d_i)) \quad (5)$$

How might the Internet be described? \n A maze – a bewildering labyrinth, easy to enter, hard to exit, multiple paths to choose, few sign posts to trust, no visible organization, makes one wonder why one entered in the first place. \n A jungle – emphasis on the danger, have to hack to get in, hack to get through, hack to get out, all the while carrying your pistol in one hand in case a lion or tiger or bear pounces on you (OK, I know bears don't do jungles and don't pounce, but don't bicker with my metaphor). \n A party – where you don't know many, weave your way through the little clusters of partyers, stop and talk to one or another, hope to find a corner to enjoy, a friendly face to chat with. \n A tool – to get a job done, with lots of buttons and gauges and levers, the insides of which one really doesn't want to see, sometimes more bother than it's worth, without an owner's manual, which one probably wouldn't read anyway, and not much way to measure how effective a job one is

Color Legend: 1 step 2 steps 3 steps 4 steps

Figure F.7: Model trained with CYB loss produces variable pause durations on tokens.

Using the definition (1), we notice that

$$\begin{aligned}
d_i \tilde{\omega}_i + (1 - d_i) &= \frac{1}{\sum_{k=i}^{W^{\max}} \omega_k} \left(d_i \omega_i + (1 - d_i) \sum_{k=i}^{W^{\max}} \omega_k \right) \\
&= \frac{1}{\sum_{k=i}^{W^{\max}} \omega_k} \left(d_i \omega_i + \omega_i - d_i \omega_i + (1 - d_i) \sum_{k=i+1}^{W^{\max}} \omega_k \right) \\
&= \frac{1}{\sum_{k=i}^{W^{\max}} \omega_k} \left(\omega_i + (1 - d_i) \sum_{k=i+1}^{W^{\max}} \omega_k \right)
\end{aligned}$$

Moreover, we also notice that

$$\prod_{j=1}^{i-1} (1 - \tilde{\omega}_j) = \prod_{j=1}^{i-1} \frac{\sum_{k=j+1}^{W^{\max}} \omega_k}{\sum_{k=j}^{W^{\max}} \omega_k} \quad (6)$$

$$= \frac{\prod_{j=1}^{i-1} \sum_{k=j+1}^{W^{\max}} \omega_k}{\prod_{j=1}^{i-1} \sum_{k=j}^{W^{\max}} \omega_k} \quad (7)$$

$$= \left(\sum_{k=i}^{W^{\max}} \omega_k \right) \left(\frac{1}{\sum_{k=1}^{W^{\max}} \omega_k} \right) \left(\frac{\prod_{j=2}^{i-1} \sum_{k=j}^{W^{\max}} \omega_k}{\prod_{j=2}^{i-1} \sum_{k=j}^{W^{\max}} \omega_k} \right) \quad (8)$$

$$= \sum_{k=i}^{W^{\max}} \omega_k, \quad (9)$$

where we used the fact that $\sum_{k=1}^{W^{\max}} \omega_k = 1$. Now, we plug these two into (5) and we get

$$\Pr(S = i | \mathbf{d}, \boldsymbol{\omega}) = \left(\prod_{j=1}^{i-1} d_j \right) \left(\omega_i + (1 - d_i) \sum_{k=i+1}^{W^{\max}} \omega_k \right) \quad (10)$$